



Evaluating the Practicability of Multiphase CFD for BWR Fuel Assembly Analysis

April 2017

Changing the World's Energy Future

Su-Jong Yoon, Giulia Agostinelli, Emilio Baglietto



INL is a U.S. Department of Energy National Laboratory operated by Battelle Energy Alliance, LLC

DISCLAIMER

This information was prepared as an account of work sponsored by an agency of the U.S. Government. Neither the U.S. Government nor any agency thereof, nor any of their employees, makes any warranty, expressed or implied, or assumes any legal liability or responsibility for the accuracy, completeness, or usefulness, of any information, apparatus, product, or process disclosed, or represents that its use would not infringe privately owned rights. References herein to any specific commercial product, process, or service by trade name, trade mark, manufacturer, or otherwise, does not necessarily constitute or imply its endorsement, recommendation, or favoring by the U.S. Government or any agency thereof. The views and opinions of authors expressed herein do not necessarily state or reflect those of the U.S. Government or any agency thereof.

Evaluating the Practicability of Multiphase CFD for BWR Fuel Assembly Analysis

Su-Jong Yoon, Giulia Agostinelli, Emilio Baglietto

April 2017

**Idaho National Laboratory
Idaho Falls, Idaho 83415**

<http://www.inl.gov>

**Prepared for the
U.S. Department of Energy
Under DOE Idaho Operations Office
Contract Unknown**

Evaluating the Practicability of Multiphase CFD for BWR Fuel Assembly Analysis

Su-Jong Yoon^{1*}, Giulia Agostinelli² and Emilio Baglietto²

¹ Idaho National Laboratory: 2525 Fremont Ave., Idaho Falls, Idaho, 83415, and sujung.yoon@inl.gov

² Department of Nuclear Science and Engineering, Massachusetts Institute of Technology: 77 Massachusetts Ave. Cambridge, Massachusetts, 02139

Abstract – Multiphase computational fluid dynamics (M-CFD) models of a boiling water reactor (BWR) fuel assembly have been generated in the commercial CFD code, STAR-CCM+ Ver.11.04.010-R8. The Eulerian multiphase approach was employed, in combination with a baseline ‘Zero Closure model’ for two-phase flow boiling, applicable to high void fraction regimes. The capability and practicability of M-CFD for BWR fuel assembly were evaluated against the international OECD/NRC BWR Full-size Fine-mesh Bundle Test (BFBT) benchmark data. The benchmark selected, BFBT-4101-61, is a steady-state full power case, with high void fraction conditions. Geometrical modeling and mesh construction of BWR assemblies introduce challenges in generating high quality computational meshes, while retaining a low cell count to allow acceptable runtimes. In order to evaluate the scalability of the CFD code, parallel CFD simulations were carried out with the High Performance Computing (HPC) system of the Idaho National Laboratory. M-CFD results display good agreement with the experimental data for both local void fraction distribution and exit quality. The parallel speedup factor is linearly proportional to the number of processors up to 500 cores, and retains over 92% efficiency with 1000 cores. The execution time of the simulation decreased exponentially with increasing number of processors while the cost of the simulation increased linearly. The proposed baseline closure, in combination with the parallel performance of the STAR-CCM+ code demonstrated promising capabilities for analyzing BWR fuel assemblies.

I. INTRODUCTION

Boiling Water Reactors (BWRs) are characterized by the two-phase nature of the coolant. Thus, the detailed understanding of the two-phase phenomena through a BWR fuel assembly is crucial for the accurate assessment of the reactor performance and safety. The time and costs associated with experimental research has pushed the development of numerical analysis. Computational Fluid Dynamics (CFD) provides the finest resolution by predicting flow quantities (such as void fraction or coolant velocity) at any location. For this reason, CFD codes allow the detailed analysis of the two-phase coolant flow and heat transfer phenomena in BWR cores. While CFD codes can be computationally very expensive, the Eulerian-Eulerian approach ensures the necessary model resolution while keeping the computational costs low. Any two-phase flow can be separated into one of several fields; every field is then treated as a continuum filling the entire volume and described by a set of conservation equations. For simplicity and computational economics reasons, the model here described is a two-field model, where the field identifies the phase and only two systems of conservation equations are solved, one for the liquid phase and one for the vapor phase. The so-called “Zero Closure model” is the baseline closure used in this work to model the physics at the interface between the two phases.

The international OECD/NRC BWR Full-size Fine Mesh Bundle Tests (BFBT) [1] has been selected as the reference benchmark, as it provides unique high-resolution

void fraction measurements to assess the accuracy of CFD models for two-phase flows in a BWR fuel assembly. In this paper the current capabilities of M-CFD are evaluated for BWR application, trying to evidence the key limitations on both aspects of modeling closures and numerical implementation, including computational scalability in order to allow efficient application to engineering design.

II. TWO-PHASE BOILING CLOSURE MODELS

In the Eulerian-Eulerian approach multiphase model the continuity, momentum, and energy equations are separately averaged for each phase and weighted by their respective volume fraction. The conservations of mass, momentum and energy are expressed for each phase k as:

- Mass conservation

$$\frac{\partial}{\partial t}(\alpha_k \rho_k) + \nabla \cdot (\alpha_k \rho_k \mathbf{u}_k) = \sum_i (\dot{m}_{ki} - \dot{m}_{ik}) \quad (1)$$

$$\sum_k \alpha_k = 1 \quad (2)$$

- Momentum conservation

$$\begin{aligned} \frac{\partial}{\partial t}(\alpha_k \rho_k \mathbf{u}_k) + \nabla \cdot (\alpha_k \rho_k \mathbf{u}_k \mathbf{u}_k) - \nabla \cdot (\alpha_k (\boldsymbol{\tau}_k + \boldsymbol{\tau}_k^t)) \\ = -\alpha_k \nabla p + \alpha_k \rho_k \mathbf{g} + \mathbf{M}_k \end{aligned} \quad (3)$$

▪ Energy conservation

$$\frac{\partial}{\partial t}(\alpha_k \rho_k e_k) + \nabla \cdot (\alpha_k \rho_k u_k e_k) - \nabla \cdot (\alpha_k \lambda_k \nabla T_k) = Q \quad (4)$$

The term M_k represents the sum of all the liquid-vapor interfacial forces. The interphase momentum transfer term M_k includes contributions from the drag, virtual mass, lift, turbulent dispersion and wall lubrication forces as follows:

$$M_k = F_D + F_{VM} + F_L + F_{TD} + F_{WL} \quad (5)$$

Closure equations must be provided for each of these forces. While accurate closure models that are applicable to high void fraction regimes are still lacking, the experience gained through the Numerical Nuclear Reactor project [2] allows implementing a baseline closure to evaluate the current capabilities of M-CFD. This closure aims at including the simplest and most robust representation of the key mechanisms, rather than aiming at absolute accuracy of the predictions, and is referred here as ‘Zero Closure’.

Based on the surface area of spherical particle, the interfacial area density is modeled through the use of a Sauter mean diameter d_s [3]:

$$A = 6\alpha_g / d_s \quad (6)$$

where the Sauter diameter is then varied to describe the interfacial variation among different flow regimes. Figure 1 describes the Sauter diameter variation at increasing void fraction.

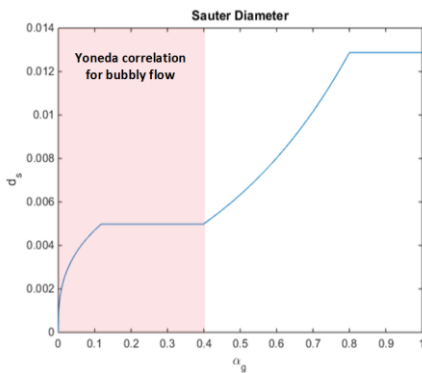


Figure 1. Sauter diameter correlation in the Zero model.

The Yoneda correlation [4] is used for the bubbly flow regime, when $\alpha_g < 0.4$. An exponential trend is chosen for the intermediate flow regimes ($0.4 \leq \alpha_g < 0.8$) and a constant value of 0.01278 for annular flow ($\alpha_g \geq 0.8$). The constant value is computed as the difference between the hydraulic diameter of the sub-channel of the fuel assembly and two times the film thickness, assumed as 1 mm. This simple approach allows treating the gas phase as the dispersed component in

annular regime, while providing a simple estimate of the interfacial area to the interfacial closures.

Accurate lift closures applicable beyond isolated configurations are still being developed and current work as evidenced the inapplicability of existing correlations [5]. In this work, the lift closure adopts the simplest possible formulation to reproduce the key physical effect of bubble migration through a simple step function. A positive and constant value of 0.025 is used for $\alpha_g < 0.25$, representing almost spherical bubbles in the low void fraction regime, which accumulate near the wall; while a negative constant value of -0.025 is used for $\alpha_g \geq 0.25$, representing larger wobbly bubbles that migrate towards the center of the channel.

Closures for drag, virtual mass, turbulent dispersion and wall lubrication have been selected following a similar approach and are summarized in Table 1.

Table 1. Zero Closure Models

Interfacial Force	Model
Lift	Step Function
Drag	Tomiyama [6]
Virtual Mass	Auton [6]
Turbulent Dispersion	FAD [6]
Wall Lubrication	Antal [6]

The inter-phase heat and mass transfers, necessary to solve the conservation of mass and energy equations, are obtained by considering the heat transfers from the gas and the liquid to the gas/liquid interface. A correlation for the Nusselt number for each phase at the interface is required to model bulk boiling and condensation. Since the difference in temperature between the interface and the vapor phase is not significant, a constant value (set to 2.0) is used for the vapor phase, which has shown not to impact the quality of the solution. The Chen-Mayinger correlation is used for the liquid phase, instead.

$$Nu = 0.185 Re_v^{0.7} Pr_l^{0.5} \quad (7)$$

In order to represent the heat transfer between the heated wall and the fluid and the boiling at the wall, a previously validate form of the classic Kurul-Podowski mechanistic heat partitioning is applied [6].

III. BFBT BENCHMARK ANALYSIS

1. CFD Modeling of BFBT Rod Bundle

The BFBT 8×8 high burn-up bundle (Type-4) consists of 60 heated rods with a single water rod in the middle of the assembly. The geometrical configuration of CFD model for the BFBT fuel bundle is shown in Figure 2. The geometric parameters of the fuel assembly are given in Table 2. Some uncertainties in the BFBT fuel assembly geometry have

been encountered. In the BFBT specification report [1], the nominal rod pitch and rod outer diameter are 16.2 mm and 12.3 mm, respectively. However, a rod pitch and spacer thickness in the 3D view in the report was 15.5 mm and 0.75 mm, respectively. Another schematic of geometric configuration in the report shows a spacer thickness of 0.5 mm and the rod outer diameter of 12 mm. In this study, the CFD model was developed based on the spacer grid geometry constructed by Neykov [7], setting the spacer thickness equal to 0.5 mm.

Simplified spacer grid geometry was employed by not including dimples and straps of the original spacer grid in the computational domain. Since the ferrule-type spacer consists of inner annuli that are in contact with each other, a contact line would characterize these locations and introduce challenges in the mesh discretization. In order to prevent poor quality mesh issues in those regions, a larger contact area was introduced, as shown in Fig. 2. The flow area variation due to these modifications is less than 0.1 %.

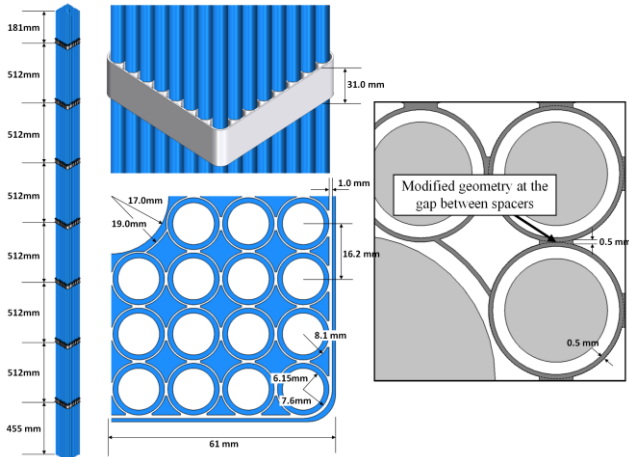


Fig. 2. Computational domain of BFBT Type-4 fuel bundle with spacer grids

Table 2. Design Parameters of BFBT Fuel Assembly

Parameters	Data
Simulated fuel assembly type	Type 4
Number of heated rods	60
Heated rod outer diameter (mm)	12.3
Heated rod pitch (mm)	16.2
Axial heated length (mm)	3708
Water rod outer diameter (mm)	34.0
Channel box inner width (mm)	132.5
Channel box corner radius (mm)	8.0
In channel flow area (mm ²)	9463
Spacer type	Ferrule

Figure 3 shows the mesh structure of the CFD model. A hexa-dominant trimmed mesh, in combination with a boundary fitted prism layer was generated with the built-in mesh generation capabilities of the STAR-CCM+ software.

The mesh adopted is relatively coarse, and was selected from separate sensitivity studies. The a uniform cell size of 2.0 mm is used away from the wall, while the prism boundary layer total thickness was specified to be 0.5 mm, and two layers are implemented to guarantees a Y+ value for the near wall cell between 30 and 100. The total number of cells is 11.42 million.

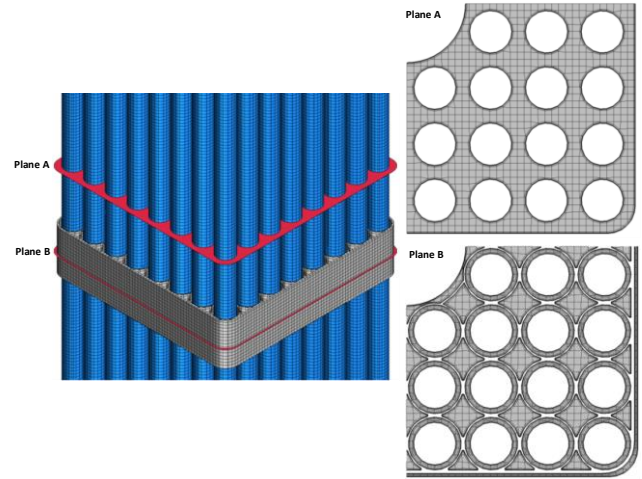


Fig. 3. Mesh structure of CFD model

Figure 4 presents cell quality metrics on two cross-sectional planes at different elevations. This cell quality metrics is based on a hybrid of the Gauss and least-squares methods for cell gradient calculation methods, which allows accounting for both the relative geometric distribution of the cell centroids of the neighbor cells and the orientation of the cell faces.

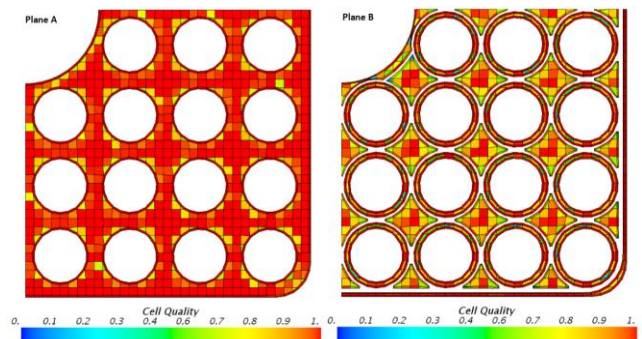


Fig. 4. Mesh qualities on the cross-sectional planes of the CFD model

The low quality of flat cells with highly non-orthogonal faces significantly influences the stability and robustness of the simulation in two-phase flow modeling. Poor quality mesh in current M-CFD solvers causes high local temperature over- and under-predictions that most often lead to large instabilities. Mesh quality is commonly difficult to get in the contact areas of spacer grids. For this reason special attention should to be paid during the computational

geometry generation to avoid creating contact points or lines. Replacing a contact line with a contact surface is usually sufficient for the improvement of the mesh quality. The minimum mesh quality of this model was approximately 0.1 and the volume-averaged mesh quality of computational domains were 0.955.

The boundary conditions of CFD model were derived from the conditions of the BFBT test 4101-61. The axial power profile in the assembly is uniform, while varying radially as shown in Fig. 5. The characteristic power distribution inside a fuel assembly is reproduced in the calculations imposing the surface heat flux for each rod with the multiplier shown in Fig. 5. The total power for the BFBT test 4101-61 case was 6.48 MW. Inlet liquid and vapor temperatures were specified as 551.096 K and 560.538K, respectively, while the operating pressure was 7.159 MPa. The inlet mass flow rate was 15.28 kg/s. The inlet velocity profile was specified as obtained from a separate fully developed single-phase flow simulation of the fuel bundle.

A (for Assembly 4, C2A, C3)							
1.15	1.30	1.15	1.30	1.30	1.15	1.30	1.15
1.30	0.45	0.89	0.89	0.89	0.45	1.15	1.30
1.15	0.89	0.89	0.89	0.89	0.89	0.45	1.15
1.30	0.89	0.89			0.89	0.89	1.15
1.30	0.89	0.89			0.89	0.89	1.15
1.15	0.45	0.89	0.89	0.89	0.89	0.45	1.15
1.30	1.15	0.45	0.89	0.89	0.45	1.15	1.30
1.15	1.30	1.15	1.15	1.15	1.15	1.30	1.15

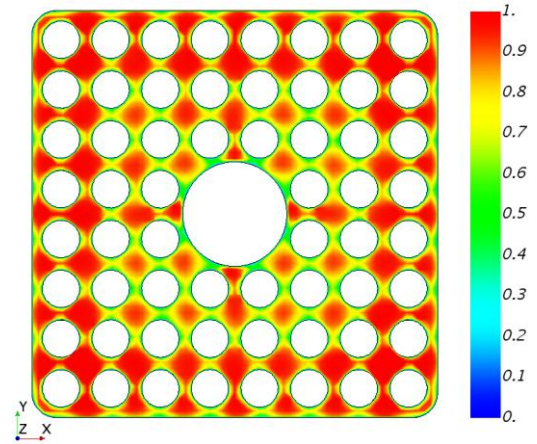
Fig. 5. Radial power distribution of test assembly type-4 [1]

2. Result of BFBT CFD Benchmark Analysis

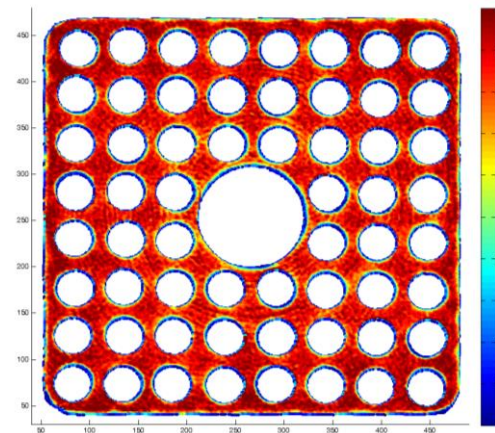
The CFD simulations have been performed with the commercially available STAR-CCM+ software, v11.04.010-R8. Evaluating numerical convergence in M-CFD requires particular attention, due to the complexity of the phase coupling through interfacial momentum and mass transfer. The residual values for the momentum and energy equations of the vapor phase decrease only to the order of 10^{-1} while those for the liquid phase decrease to the order of 10^{-3} – 10^{-4} . Convergence of the physical parameters is therefore monitored, in addition to the total mass conservation. The relative deviation of sum of the phase mass flow rates between the inlet and outlet boundaries was less than 0.3%.

The exit quality and sub-channel averaged void fraction distribution were analyzed to assess the overall predictions of the Zero closure. Figure 6 shows the void fraction distributions of CFD simulation and experiment. The CFD simulation results use a different color scale from the experiment to better appreciate the void distribution inside the subchannels. The average void fraction at the outlet

cross section for the experiment and CFD simulations are 80.64% and 80.77%, respectively. The void fraction is higher getting far from the center of the assembly as a consequence of the radial power distribution, being higher in this region. M-CFD is able to qualitatively predict the concentration of the voids in the center of each subchannel.



(a) CFD ($\alpha_{avg}=80.77\%$)



(b) Experiment ($\alpha_{avg}=80.64\%$)

Fig. 6. Comparison of void fraction distribution (BFBT 4101-61)

In order to quantitatively assess the accuracy of the CFD simulation, the predicted local void fraction is averaged in each sub-channel and then compared with the measured values in selected sub-channels. The location of the sub-channels that are selected for comparison is illustrated in Figure 7. Figure 8 shows the deviation of the sub-channel averaged void fraction between the CFD prediction and experimental data in the selected sub-channels. The maximum deviation for the sub-channel averaged void fraction is 12.93% at the outer corner of the BFBT fuel assembly (Location L). The deviation of sub-channel averaged void fraction for the other selected locations is less than $\pm 10\%$. The predicted thermal equilibrium quality at the outlet (24.49%) agrees with experiments (25%).

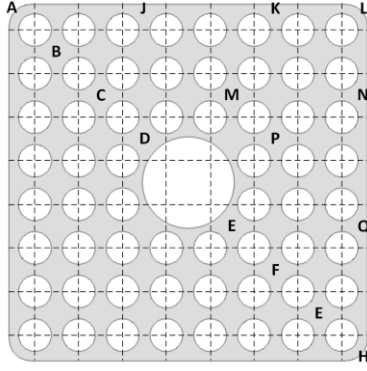


Fig. 7. Reference sub-channels location

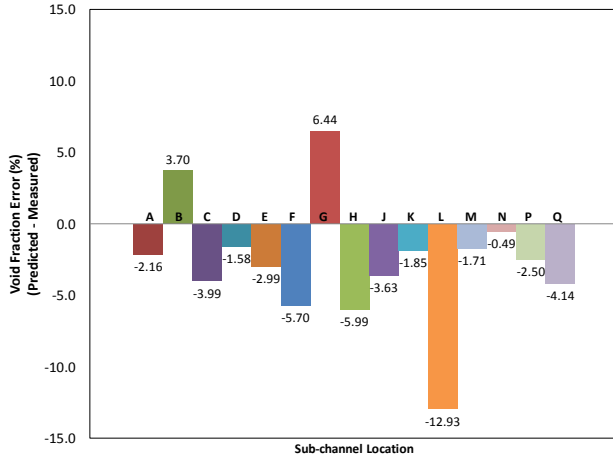


Fig. 8. Deviation of sub-channel averaged void fraction

IV. PERFORMANCE ANALYSIS OF PARALLEL COMPUTATION

An important objective of the present work has been to evaluate the computational performance of large, full assembly M-CFD models. The adopted CFD model of the BFBT fuel bundle, which is comprised of 11.42 million cells, is expected to further grow with more advanced spacer designs. The parallel performance of the CFD model therefore represents a key to the applicability of M-CFD to fuel analysis. The High Performance Computing (HPC) system, Falcon, at Idaho National Laboratory (INL) was used for all calculations. Falcon is INL's flagship cluster with over 600 TFlops of performance. The number of iterations for the simulations was specified as 3,000.

The most significant advantage of parallel computing is obviously the reduction in computational time. The Speedup factor (S) is used to express this reduction and it is defined as follows:

$$S(n) = t_s / t_n \quad (8)$$

where t_s is the execution time on a single processor and t_n is the execution time on n -processors.

Figure 9 shows the speedup factor with increasing number of processors. The speedup factor was linearly proportional to the number of processors up to 500 processors, and while slowly reducing it still provided over 92% efficiency with 1000 cores compared with 500 cores.

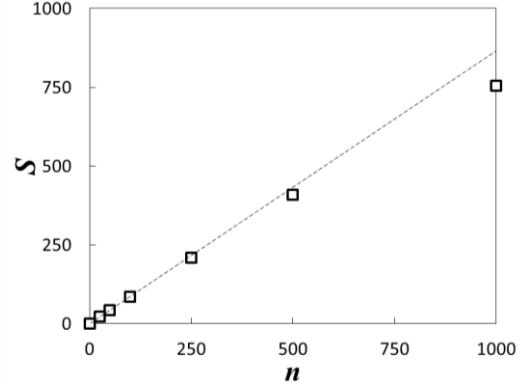


Fig. 9. Plot of speedup factor as a function of number of processors

Another measure to evaluate the performance of parallel computing is the cost of parallel computation (C). The cost is defined as a product of the number of processors used times the execution time as follows:

$$C = n \cdot t_n \quad (9)$$

where n is the number of processors.

Figure 10 shows the execution time and cost of parallel computation as a function of number of processors. The execution time of the parallel computing decreased exponentially with increasing number of processors while the cost of computation increased linearly.

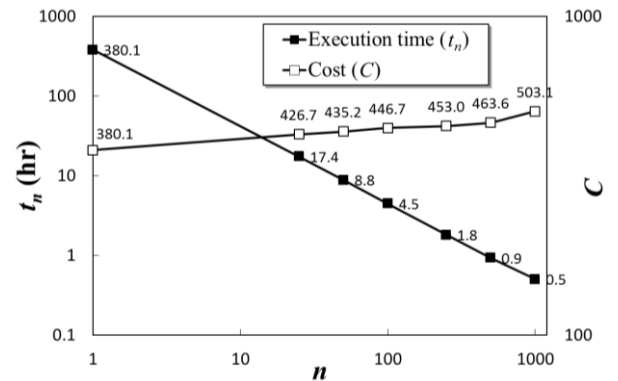


Fig. 10. Plot of execution time and cost of parallel computations

According to the definition of cost in Eqn. (9), the cost of single processor is equal to the execution time of single processor run. As for the run on a single processor, the

values of cost and execution time of running a single processor were approximately 380. The execution time with 1,000 processors was significantly reduced by 0.5 hours which is 99.86% reduction compared to a single processor run, while the cost of the computation increased by 32.37% compared that of a single processor. The benefit of parallel computing in terms of cost seems not to be significant. However the execution time was dramatically reduced by the parallel computing. All execution times with a core number greater than 250 were essentially practicable for engineering applications, therefore we recommend using a number of processors between 250 and 500.

The efficiency of parallel computing depends on the number of processors. This dependency can be evaluated by parallelizable fraction. According to Amdahl's Law [7], the parallelizable fraction is determined by:

$$f = \frac{n}{(n-1)} \left(1 - \frac{t_s}{t_n} \right) \quad (10)$$

Figure 11 shows the parallelizable fraction plotted as a function of number of processors. The STAR-CCM+ code is very parallelizable program so that most part of simulation was able to be parallelized.

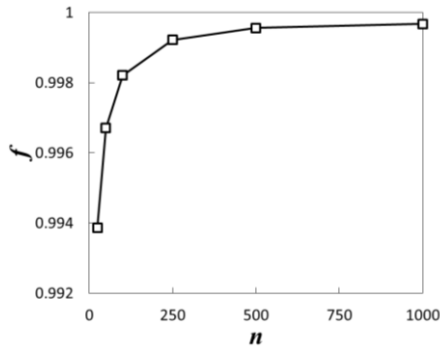


Fig. 11. Plot of parallelizable fraction as a function of number of processors

V. CONCLUSIONS

In this work, a high fidelity multiphase CFD simulation was carried out to evaluate the current capabilities of M-CFD for BWR application. The findings and conclusions are summarized as follows:

- An optimal computational model of the BFBT benchmark geometry was assembled and used for assessment of M-CFD capabilities in combination with a baseline 'Zero closure model' for the Eulerian-Eulerian physical model. Best practices are suggested to treat the geometrical complexities which allow producing high quality computational meshes.

- The high quality of the computational mesh, combined with the robust 'Zero closure model' allows good numerical convergence of the calculations.
- Both the exit quality and the local void fraction of the CFD result showed excellent agreement with the experimental data from the BFBT benchmark test case 4101-61.
- The computational time was significantly reduced by parallelization, while the cost for computation increased only marginally. Parallelization efficiency over 90% was demonstrated up to 1000 cores, while 250 to 500 cores are recommended for engineering applications.
- Based on the overall accuracy of the predictions and the excellent computational performance, it is concluded that M-CFD simulations with 'Zero Closure model' demonstrate great potential for BWR fuel analysis.

NOMENCLATURE

Latin

A	Interfacial area density
C	Cost
d_s	Sauter mean diameter
e	Enthalpy
F	Force
f	Parallelizable fraction
g	Gravitational acceleration
M	Sum of the interphase forces
\dot{m}_{ik}	Mass transfer from i-th phase to k-th phase
n	Number of processors
p	Pressure
Q	Interphase heat transfer
S	Speedup factor
T	Temperature
t_n	Execution time of n-processors
u	fluid velocity

Greek

α	Volume fraction
λ	Thermal conductivity
ρ	Density
τ	Molecular stress
τ'	Turbulent stress

Subscripts

g	Vapor phase
k	k-th phase
D	Drag force
VM	Virtual mass force
L	Lift force
TD	Turbulent dispersion force
WL	Wall lubrication force

ACKNOWLEDGMENTS

This work was supported by the Consortium for Advanced Simulation of Light Water Reactor, an Energy Innovation Hub for Modeling and Simulation of Nuclear Reactors under U.S. Department of Energy Contract No. DE-AC05-00OR22725.

REFERENCES

1. B. NEYKOV, F. AYDOGAN, L. HOCHREITER, K. IVANOV, H. UTSUNO, K. KASAHARA, E. SARTORI and M. MARTIN, NUPEC BWR Full-size Fine-mesh Bundle Test (BFBT) benchmark, Volume I: Specification, OECD, Nuclear Energy Agency, NEA No. 6212, ISBN 92-64-01088-2 (2006).
2. A. TENTNER, S. LO, A. IOILEV, V. MELNIKOV, M. SAMIGULIN, V. USTINENKO, and S. MELNIKOVA, "Computational fluid dynamics modeling of two-phase flow topologies in a Boiling Water Reactor fuel assembly," *Proceedings of the 16th International Conference on Nuclear Engineering ICONE16*, Orlando, Florida, May 11-15 (2008).
3. M. ISHII and T. HIBIKI, *Thermo-Fluid Dynamics of Two-Phase Flow*, Springer (2006).
4. K. YONEDA, A. YASUO and T. OKAWA. "Flow structure and bubble characteristics of steam-water two-phase flow in a large-diameter pipe," *Nuclear Engineering and Design*, Vol. 217, pp. 267-281 (2002).
5. R. SUGRUE and E. BAGLIETTO, A reevaluation of the lift force in Eulerian multiphase CFD. The 16th International Topical Meeting on Nuclear Reactor Thermal Hydraulics NURETH-16, September, Chicago, Illinois, (2015).
6. E. Baglietto, M.A. Christon, 2013 - "Demonstration & Assessment of Advanced Modeling Capabilities for Multiphase Flow with Sub-cooled Boiling", CASL Technical Report: CASL-U-2013-0181-001, December 23, (2013).
7. B. NEYKOV, Development and validation of advanced CFD models for detailed predictions of void distribution in a BWR bundle, Ph.D dissertation, The Pennsylvania State University, (2010).